· Article ·
doi: 10.13679/j.advps.2016.4.00272

Advances in Polar Science
December 2016 Vol. 27 No. 4: 272-279

A preliminary dayglow model for summer auroral images from Polar/UVI

WANG Lingmin[1,2] & LUAN Xiaoli[1,2,3*]

[1] CAS Key Laboratory of Geospace Environment, School of Earth and Space Sciences, University of Science and Technology of China, Hefei 230026, China;

[2] Mengcheng National Geophysical Observatory, University of Science and Technology of China, Hefei 230026, China;

[3] Collaborative Innovation Center of Astronautical Science and Technology, Harbin 150000, China

Received 12 July 2016; accepted 10 December 2016

Abstract In this study, we developed a summer dayglow model using auroral emissions acquired by the ultraviolet imager (UVI) onboard the Polar satellite. In the summer polar region, dayglow varies as a cosine-like function of the solar zenith angle (*SZA*). The shape of this function can be characterized by its amplitude (*Amp*) and phase (*Phi*) factors. We first obtained the hourly *Amp* and *Phi* factors in summers from 1996 to 2000, and then investigated the universal time (UT) and solar activity variations of these two shape factors. It was found that both factors were non-linearly dependent on the solar flux for all years, and the *Amp* factor showed clear UT variations under both low and high solar flux years. Thus, a dayglow model was constructed to consider the above dependencies. After the dayglow was removed automatically from the original UVI images via our model, the remaining auroral precipitation energy flux was in good agreement with previously reported magnetic local time–latitude (MLT–MLAT) patterns. Our model provides a fast way to statistically process summer auroral precipitation of Polar/UVI and its variations.

Keywords **dayglow in auroral images, auroral precipitation, dayglow model, Polar/UVI**

Citation: Wang L M, Luan X L. A preliminary dayglow model for summer auroral images from Polar/UVI. Adv Polar Sci, 2016, 27: 272-279, doi: 10.13679/j.advps.2016.4.00272

1 Introduction

The aurora is a phenomenon in the upper atmosphere in which particles precipitate from space and collide with atoms or molecules. It usually appears in a continuous ring surrounding the magnetic poles, which is called the auroral oval[1-2], and has been observed by ground-based instruments since 1960–1970s[3]. Although such instruments generally had high spatial resolution, they were incapable of providing global auroral information, such as the overall oval configuration and the spatial distribution of auroral intensity along the oval. Therefore, to investigate global auroral variations, there is a great advantage in using auroral emission data from imagers aboard satellites. Liou et al.[4-5] used global images acquired by the ultraviolet imager (UVI) onboard the NASA Polar satellite to investigate the global aurora pattern and its seasonal variations. Newell et al.[6] and Shue et al.[7] also used UVI images to study auroral precipitation power during substorms and the influence of the interplanetary magnetic field on global auroral patterns. It is known that auroral images acquired by the UVI onboard the Polar satellite are usually contaminated by dayglow, which is mainly produced by energetic photoelectron impact excitation of molecular nitrogen, whereas the aurora is caused by energetic particle impact excitation. Dayglow is especially strong in summer owing to a small solar zenith angle (*SZA*). Thus, an important step in processing UVI data is to determine dayglow and remove it. However, the data processing team of Polar/UVI does not provide a valid means to do so in the UVI images released to the public.

* Corresponding author, E-mail: luanxl@ustc.edu.cn

For example, the UVI data processing software (http://solar-b.msfc.nasa.gov/ssl/PAD/sppb/UVI/software/studio/) only includes a cosine-like function with fixed amplitude (*Amp*=76) and phase (*Phi*=0.83) factors. Given the lack of a dayglow model, researchers sometimes have to determine dayglow contamination and remove it from individual auroral images within a huge database. In this database, the Polar/UVI auroral emission images have a temporal resolution within 1 min[4]. This greatly limits statistical study of auroral variations using Polar/UVI, especially in summer, so a large proportion of works have used Polar/UVI images to do event studies[8-10]. In the present study, we developed a dayglow model that can determine and remove dayglow automatically from original auroral images of Polar/UVI. A preliminary dayglow model was constructed for summer, when dayglow is the most prominent.

2 Data and analysis method

The Polar satellite is designed to study the magnetosphere and aurora. It was launched on 24 February 1996 into a highly elliptical polar orbit with high inclination (78.94°) and perigee/apogee of 3125/55113 km. It continued operations until the program was terminated in April 2008. There were numerous instruments aboard the satellite, including a UVI imager, which was mainly used to study the global aurora phenomenon. The UVI could provide about 2300 images per day during each orbital period of 18 h. There were four major narrowband filters on UVI, two atomic oxygen lines centered at 1304 and 1356 Å and two molecular nitrogen Lyman-Birge-Hopfield (LBH) bands centered at 1500 Å (LBHs) and 1700 Å (LBHl)[11]. In our study, 36-s integrated images from the LBHl band were used because of a larger signal-to-noise ratio. LBHl band emission is considered to be proportional to the energy flux of auroral precipitation; therefore we used data from that band. Thus, the auroral energy flux (units: ergs·cm^{-2}·s^{-1}) can be inferred from observed LBHl intensities (units: photons·cm^{-2}·s^{-1}) by multiplying a factor of 30.2/110, as suggested by Liou et al.[5] and Newell et al.[6]

We assumed the dayglow emissions to be mainly produced by energetic photoelectron impact excitation of molecular nitrogen, which is different from aurora. The aurora is caused by energetic particle impact excitation. The dayglow depends nonlinearly on the photoelectron flux, which is related to the *SZA* according to Prinz et al.[12] Those authors indicated that the LBH emission rate was primarily dependent on the *SZA*, which varied as a cosine-like function.

Before establishing the dayglow model, we had to extract the dayglow from UVI images. First, LBHl band emissions at magnetic latitude (*MLAT*)<60° are considered dayglow noise. This noise outside the auroral oval are binned by their *SZA* on a *SZA* grid of 1°, and average dayglow is obtained in each bin. Then, the average dayglow is fitted as a function of *SZA* using the following equation, as suggested by Liou et al.[4-5]:

$$Dayglow = Amp \times \cos^2(Phi \times SZA) \quad (1)$$

Here, *SZA* is that corresponding to a dayglow pixel, and *Amp* and *Phi* are amplitude and phase, respectively.

Figure 1 shows an example of how to determine the dayglow for an original UVI LBHl band image derived from STUDIO (http://solar-b.msfc.nasa.gov/ssl/PAD/sppb/UVI/software/studio/) software at 05:05:00 universal time (UT) on 9 July 1997. The raw UVI image is compared with that after dayglow noise is removed via Equation (1) in geomagnetic coordinates (Figure 1a). In this case, Figure 1b shows that the dayglow is binned within a *SZA* range of 55°–120°, which is at *MLAT*<60°. Thus, it is completely outside the auroral oval shown in Figure 1a. In Figure 1b, the fitted curve from Equation (1) is in good agreement with the average dayglow. The fitted *Amp* and *Phi* factors for this case are 8.07 ergs·cm^{-2}·s^{-1} and 0.84, respectively. By comparing the raw map with that after dayglow removal (Figure 1a), it is clear that the dayglow noise is generally effectively removed, especially on the dayside. This shows that Equation (1) can reflect the average distribution and intensity of dayglow.

We used the LBHl images acquired by Polar/UVI during summers from 1996 to 2000 to construct the dayglow model. The summer is defined within 91 d centered on the solstice day. Only images with polar orbit altitude>6*L* (where *L* is the earth's radius) were used, so each selected image covered most of the auroral oval. For each summer, the UVI images were collected each hour, and hourly-average *Amp* and *Phi* were determined from the procedure above. These hourly values were considered observational dayglow shape factors and used to build the dayglow model. The solar cycle and UT variations of these shape factors were examined.

3 Results and discussion

In this section, we investigate the solar cycle and UT variations of the *Amp* and *Phi* factors of the dayglow. First, solar cycle effects were studied. Using the entire database for summers of 1996–2000, the correlation coefficient between *Amp* and solar flux index $F_{10.7}$ was found to exceed 0.9. Therefore, the dayglow was significantly dependent on solar activity. Second, there was a clear UT variation of dayglow *Amp* factor during 1996–2000. These results are elaborated later. On basis of these variations, the Polar/UVI dayglow model was constructed. In this model, the dayglow amplitude factor *Amp* (*Dayglow_Amp*) is expressed as functions of solar activity and UT, and the dayglow phase factor *Phi* (*Dayglow_Phi*) is expressed as a function of solar activity, as follows.

$$Daylow\_Amp = Amp_1(F_{10.7})(1+Amp_2(UT)), \quad (2)$$

$$Daylow\_Phi = Phi_1(F_{10.7}). \quad (3)$$

Detailed expressions of Amp_1, Amp_2, and Phi_1 are given explicitly:

$$Amp_1(F_{10.7}) = a_0 + a_1 \times F_{10.7} + a_2 \times F_{10.7}^2, \quad (4)$$

$$Amp_2(UT) = \sum_{j=1}^{4}\left(b_j \times \cos\left(\frac{2\pi j(UT - c_j)}{24}\right)\right), \quad (5)$$

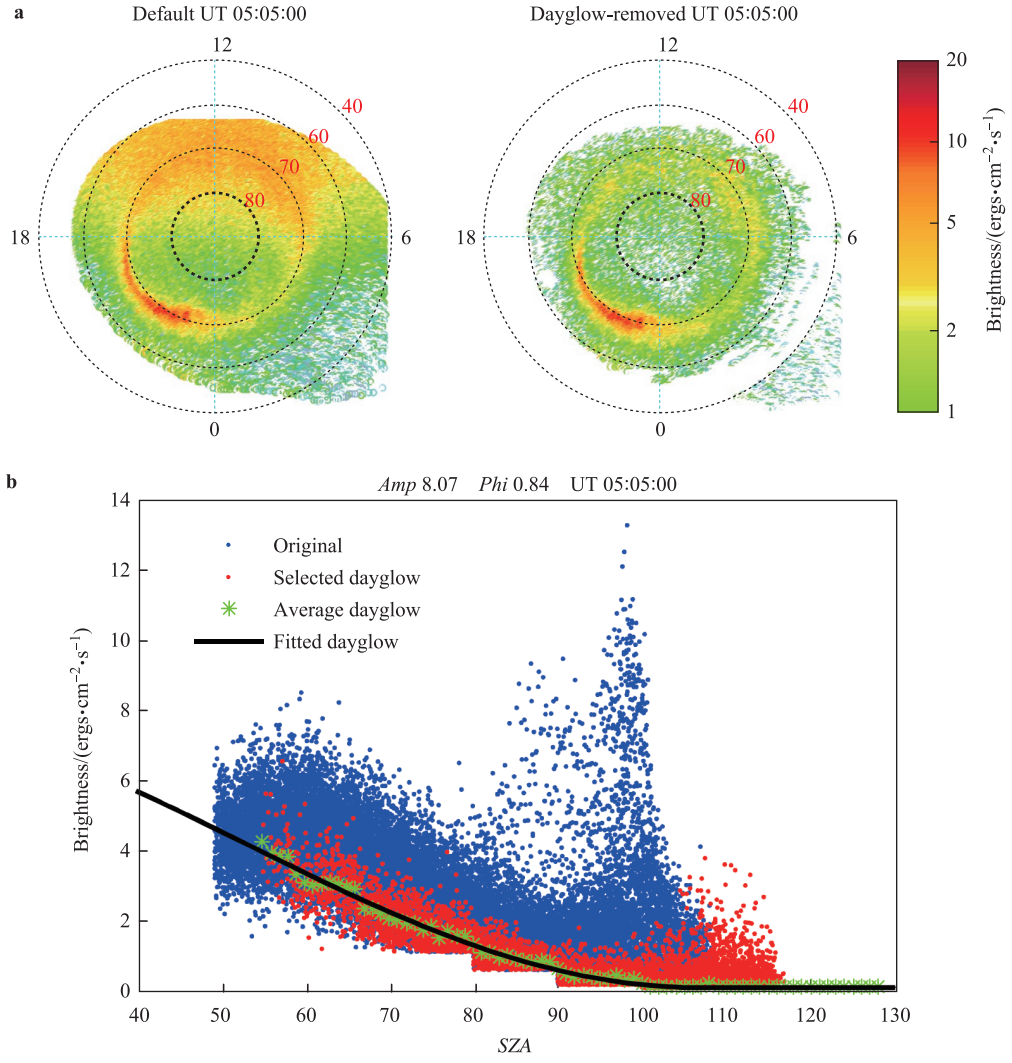

Figure 1 Comparison of raw UVI image (units: ergs·cm^{-2}·s^{-1}) with that after dayglow noise removal on 9 July 1997 in Apex coordinate (**a**). Selected dayglow noise at MLAT ≤ 60 degrees and fitted line using the form Dayglow = $Amp\times\cos^2(Phi\times SZA)$, where *SZA* is that corresponding to dayglow pixel and *Amp* and *Phi* are dayglow shape factors for amplitude and phase, respectively (**b**). Those two factors determine the fitted line. More detail is in the text.

$$Phi(F_{10.7}) = a_3 + a_4 \times F_{10.7} + a_5 \times F_{10.7}^2 . \quad (6)$$

Here, a_i, b_j, and c_j (i=0–5; j=1–4) are coefficients calculated by least-squares fit. j is equal to 1, 2, 3, or 4, and represents the first four order Fourier components with periods 24, 12, 8, and 6 h, respectively. b_j and c_j are corresponding amplitudes and phases of each Fourier component of the *Amp* factor, and π =3.1416. The values of a_i are listed in Table 1, and those of b_j and c_j are in Table 2.

Table 1 Values of nonlinear coefficients a_i for *Amp* (Amp_1) and *Phi* (Phi_1) in the equations $Amp_1(F_{10.7}) = a_0 + a_1 \times F_{10.7} + a_2 \times F_{10.7}^2$, and $Phi(F_{10.7}) = a_3 + a_4 \times F_{10.7} + a_5 \times F_{10.7}^2$.

	Coefficient		
$Amp_1(F_{10.7})$	$a_0 = -1.06\times10$	$a_1 = 5.51\times10^{-1}$	$a_2 = -9.00\times10^{-4}$
$Phi_1(F_{10.7})$	$a_3 = 7.90\times10^{-1}$	$a_4 = 2.00\times10^{-4}$	$a_5 = -9.00\times10^{-7}$

Table 2 Values of amplitude (b_j) and phase (c_j) for each of first four order Fourier components of average *Amp* (Amp_2) for summers from 1996 to 2000. Fourier components are for periods 24, 12, 8 and 6 h

	Period=24	Period=12	Period=8	Period=6
Amplitude (b_j)	4×10^{-2}	1.95×10^{-2}	1.57×10^{-2}	8.50×10^{-3}
Phase (c_j)	−2.98	−4.70	2.86	−1.94

Values of the coefficients a_i, b_j, and c_j were used to construct the model for the two dayglow shape factors for each summer of 1996–2000. Equations (2)–(6) consider the solar flux dependence of *Amp* and its variations with UT. An average UT variation pattern (Amp_2) was determined for these five years. These solar cycle and UT variations of *Amp* are discussed later.

Model–data comparisons of *Amp* (top five panels) and percentage differences between model and data (bottom five panels) are shown in Figure 2 for each summer of 1996–2000. We made similar comparisons for shape factor *Phi* in Figure 3. Daily means of *Amp* (green dots) and average percentage differences (<Δ>) each summer are also given. As shown in top five panels of Figure 2, the observed dayglow *Amp* generally clusters near model values. The latter values are generally consistent with daily means (green dots) of *Amp*. There are inconsistencies during some shorter periods, such as day 196 to 216 in 2000 and day 186 to 196 in 1998, for which the model underestimated the observations. The top five panels in Figure 3 show that the modeled dayglow *Phi* factor is also generally consistent with observed. Model *Phi* values are close to daily means (green dots) in all summers, except for an overestimation in August 1996 (around days 190–218).

In the bottom five panels of Figures 2 and 3, the average percentage differences in summers of 1996–2000 are about −17.6%, 0.8%, 7.7%, 0.8%, and −3.3% for *Amp*. Corresponding standard deviations of the percentage differences in summers 1996–2000 are about 21.3%, 20.6%, 15.2%, 11.4%, and 16.4%. It is obvious that averages of the percentage differences (<Δ>) are random error, from the standard deviations of these five years. This suggests that the model could generally reproduce the dayglow emission *Amp* factor well each summer, except 1996. Average differences

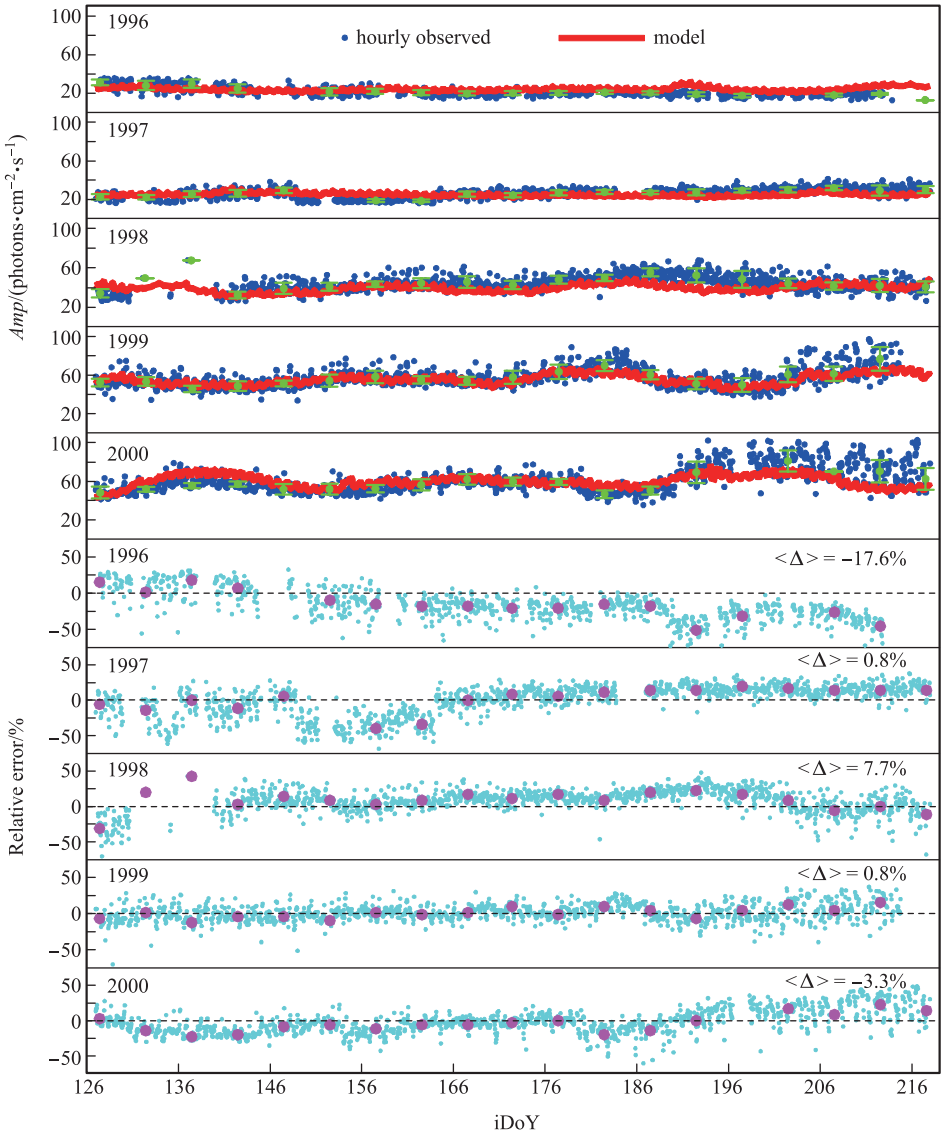

Figure 2 Comparison of model *Amp* with hourly observations (top five panels) and percentage differences between the two (bottom five panels). Percentage difference was calculated by $\Delta(\%) = \frac{observation - model}{observation} \times 100$. Daily means of observed *Amp* and percentage difference are also shown, in top five (green dots) and bottom five (magenta dots) panels, respectively. <Δ> is average percentage difference each summer.

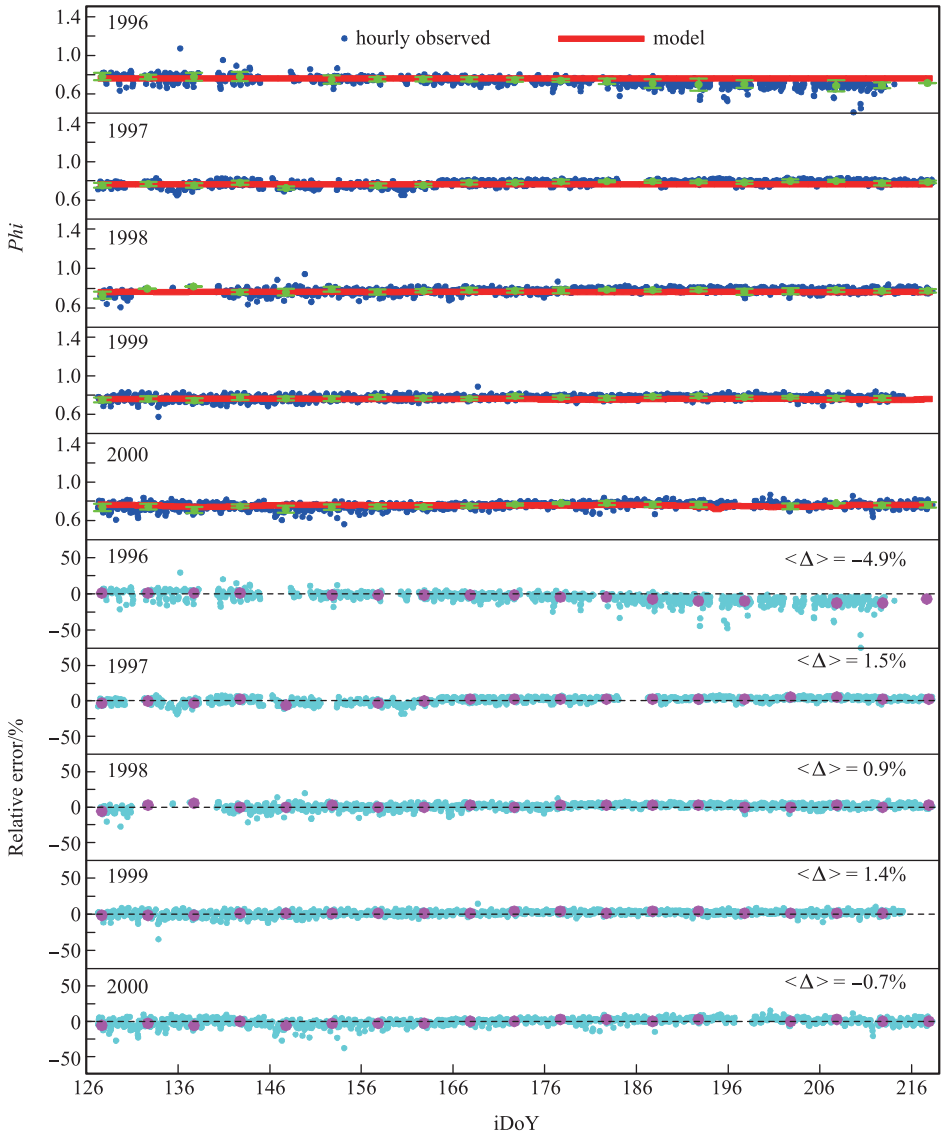

Figure 3 Same as Figure 2, but for dayglow phase factor of *Phi*.

between observed and model *Phi* values are <5% for all summers. In addition to the *Amp* factor, the dayglow emission value depends on the *SZA*. If typical *SZA*s of 65° and 100° are used for daytime and nighttime sectors respectively, as shown in Figure 1b, values of the cosine-like function (i.e., $\cos^2(Phi \times SZA)$) are 0.38 and 0.03 for the dayside and nightside sectors, respectively. The *Phi* value is estimated at 0.8. As a result, the average uncertainty of −17.6 % in the summer *Amp* factor of 1996 would introduce absolute uncertainties in dayglow emissions of ~0.37 ergs·cm^{-2}·s^{-1} in the dayside sector and <0.03 ergs·cm^{-2}·s^{-1} for the nightside. Average auroral precipitation energy fluxes are about 2 and 2.5–3 ergs·cm^{-2}·s^{-1} for dayside and nightside, respectively. Thus, the average uncertainty of our model dayglow values each summer are <~20% of the auroral energy in dayside, and can be ignored for nightside as compared with the auroral intensity. Therefore, our model is reasonably effective at extracting the auroral feature from UVI images, especially in the nightside.

Regarding the uncertainty of hourly *Amp* values, the percentage differences were mostly < 25% in solar maximum years and sometimes reached 50% in 1996 and 1997. In those two solar minimum years, this percentage difference could introduce an absolute uncertainty as large as ~0.48 ergs·cm^{-2}·s^{-1} in hourly dayside dayglow values. This could affect the auroral feature extracted in dayside from individual images. Larger observation/model differences may be associated with fast variations of $F_{10.7}$ values, auroral activities, and the line of sight direction of the satellite.

Using a_i coefficients and Equations (4) and (6), the model dayglow shape factors of *Amp* and *Phi* were calculated as a function of $F_{10.7}$. Figure 4 shows solar cycle variations of the model and observational daily dayglow shape factors of *Amp* (top panel) and *Phi* (bottom panel). In this figure,

the model and observational data show generally good agreement. In Table 1, a_i (i=2, 5) is close to zero, suggesting that dayglow *Amp* and *Phi* vary almost linearly with solar flux. From Figure 4, the *Amp* factor of the dayglow increases strongly with the solar flux. This suggests a strong control of solar flux on dayglow in the UVI images. However, there is a relatively stable *Phi* value ~0.8 in all solar activity conditions. There is only a weak negative correlation (coefficient = −0.2) between *Phi* and $F_{10.7}$. The *Phi* factor slightly decreases with increase of $F_{10.7}$. Figure 4 also shows the standard deviation of observational daily *Amp* and *Phi* values on a $F_{10.7}$ grid of 20 for low-to-moderate solar flux, and of 40 for strong solar flux. These deviations are in the range 1.80–9.60 photons·cm^{-2}·s^{-1} for *Amp* and 0.01–0.03 for *Phi*.

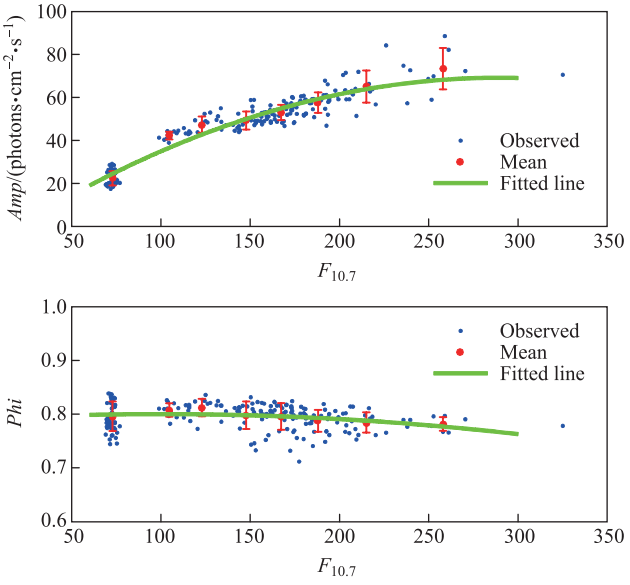

Figure 4 Solar cycle dependence of dayglow shape factors of *Amp* (top panel) and *Phi* (bottom panel). Observed *Amp* and *Phi* are daily means of hourly derived values. Red dots with error bars show means of *Amp* and *Phi* on a $F_{10.7}$ grid of 20 for low-to-moderate solar flux, and of 40 for strong solar flux. Error bars show standard deviation.

Clear and similar relative UT variations of the *Amp* factor were obtained using Equations (2) and (5) for the summers of 1996–2000. This UT pattern is relative to the solar cycle variations of *Amp* according to Equation (2). Figure 5 portrays relative UT variations of *Amp* (Amp_2) in summers of 1996–2000, as well as average relative UT variation during the five years. This variation was used in our dayglow model. As seen in Figure 5, the dayglow shape factor of *Amp* had an obvious UT variation each summer. It shows that the average relative *Amp* clearly varied with UT and reached its maximum (~0.06) and minimum (~−0.05) around 13:00 and 20:00 UT, respectively. This suggests a UT variation amplitude ~11% for *Amp* relative to its daily mean. According to Table 2, the diurnal Fourier component contributed most to the UT variations of *Amp*, because its amplitude was the largest. This might be associated with the departure of the magnetic pole from the geographic pole.

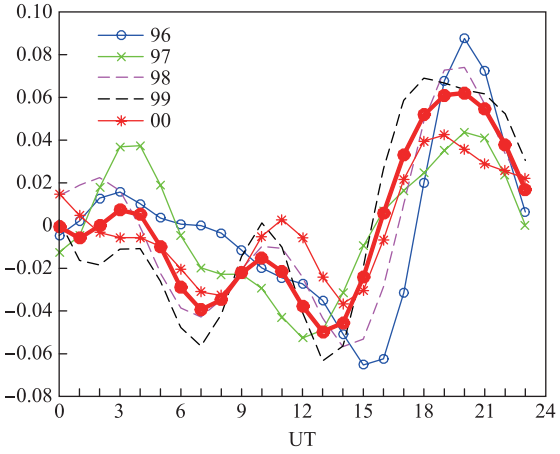

Figure 5 Average relative UT variation ($Amp_2(UT)$), red circled of dayglow *Amp* factor during all summers from 1996 to 2000, and its pattern each summer. $Amp_2(UT) = \sum_{j=1}^{4}\left(b_j \times \cos\left(\frac{2\pi j(UT - c_j)}{24}\right)\right)$.

To further validate our dayglow model, Figure 6 shows an average auroral energy flux pattern at 06:00 UT after dayglow was removed by our model, under *Kp*=2 conditions in summer 1997. This result is similar to the average summer pattern obtained by Liou et al.[4], who showed that auroral emission peaks generally occurred in three different regions of the northern auroral oval during summer. These peaks include the most intense emissions centered at ~22:30 MLT and ~68° MLAT, a weaker one centered at ~15:00 MLT and ~75° MLAT, and a much weaker one centered around 09:00 MLT. Their relative intensities varied from May through July. All these peaks can be seen clearly in the auroral oval of Figure 6. At locations in the nightside polar cap and latitudes lower than ~64° MLAT, which are outside the auroral oval, the dayglow has been effectively removed. These results illustrate that our dayglow model is feasible and performs well in modeling the average dayglow in summer auroral images.

The above results show that the dayglow has a near constant *Phi* factor of ~0.8. This factor exhibits a weak solar cycle variation, which has a maximum ~0.80 at solar minimum ($F_{10.7}$=70) and minimum ~0.78 at solar maximum ($F_{10.7}$=250). The dayglow *Amp* factor is largely dependent on solar activity, with a maximum ~70 photons·cm^{-2}·s^{-1} at solar maximum ($F_{10.7}$=250) and minimum ~25 photons·cm^{-2}·s^{-1} at solar minimum ($F_{10.7}$=70). The shape factor *Amp* of dayglow also had a clear UT variation under both high and low solar flux years 1996—2000. These findings may be attributed to the departure of the geomagnetic and geographic poles, because of which the auroral oval can be found in different geographic locations in different UT hours. Therefore, the

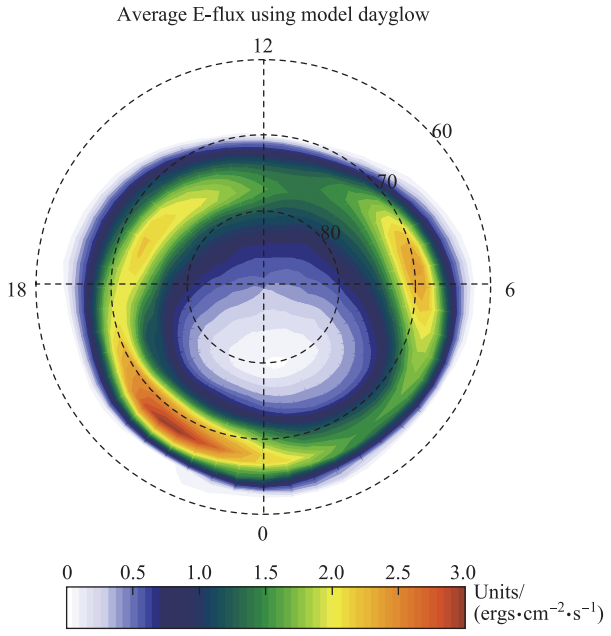

Figure 6 Average auroral energy flux at UT=06:00 in summer 1997, under *Kp*=2 conditions.

solar flux and consequent dayglow over the auroral oval vary with UT.

The difference between modeled and observed dayglow *Amp* could be from various sources, such as the look angle of the UVI and geomagnetic activity. The boundary of the auroral oval is affected by geomagnetic/auroral activity. When that activity increases, the boundary moves to a lower *MLAT*. In our study, a fixed *MLAT* of 60 degrees was assumed to be the equatorward auroral oval boundary. Hence, under intense geomagnetic activity, the selected dayglow emissions may have been mixed with auroral precipitation. However, because solar flux is the dominant determinant of dayglow in summer, these phenomena would have little influence on the average dayglow pattern in summer during most years, especially for the nightside. Nevertheless, the results in Figure 6 indicate that when the average energy flux pattern is obtained after dayglow removal by our model, it is consistent with previously reported results. For any individual image, a relative uncertainty as much as ~50% and absolute uncertainty as much as ~0.48 ergs·cm^{-2}·s^{-1} may occur for the dayglow *Amp* factor and dayside dayglow emission, respectively. Our future work will investigate seasonal variations of the dayglow, which can augment auroral statistics for entire years.

4 Summary

In the present study, we constructed a dayglow model based on LBHl band images acquired by Polar/UVI during summers of 1996–2000. This model considers dayglow that is principally excited by photoelectrons as a cosine-like function of the *SZA*, which varies with UT and solar activity (as measured by the $F_{10.7}$ index). That function is characterized by its *Amp* and *Phi* factors, which can be used to remove dayglow from raw UVI images to extract auroral emissions. The main results are as follows.

1. Dayglow *Amp* factor from UVI images increases nonlinearly with solar activity. It is ~20–30 photons·cm^{-2}·s^{-1} at solar minimum ($F_{10.7}$=70), increasing to ~70 photons·cm^{-2}·s^{-1} at solar maximum ($F_{10.7}$=250).

2. The dayglow *Amp* factor had obvious UT variation under both low and high solar flux years during 1996–2000. During those years, the average relative UT variation amplitude was ~11% as compared with its daily mean.

3. A dayglow model was constructed based on the dependence on solar activity and UT hours of dayglow *Amp* and *Phi* factors. Generally, this model reproduced well the dayglow *Phi* and *Amp* observed by Polar/UVI in summers.

4. The dayglow *Phi* and *Amp* factors had an average uncertainty <17.6% for all summers. In that season, average uncertainties of model dayglow values were <~20% in the dayside and could be ignored in the nightside. There was absolute uncertainty of dayside dayglow emissions values as large as ~0.48 ergs·cm^{-2}·s^{-1} in individual images.

5. After using the model to aomatically remove dayglow in UVI images, the remaining auroral precipitation energy flux agreed well with previously reported results of the MLT–MLAT pattern.

The Polar/UVI produced auroral emission images with temporal resolution within 1 min, accumulating a huge number of images. To obtain summer auroral energy flux maps in the polar region, researchers in the past typically had to manually remove dayglow within the map for each image. Our model provides a fast means to quantitatively process summer auroral precipitation of Polar/UVI, so it will greatly benefit the analysis of auroral variations, especially in statistical investigations.

Acknowledgments The Polar/UVI data were downloaded from the website ftp://cdaweb.gsfc.nasa.gov/pub/data/polar/uvi/uvi_level1/. We thank NASA for providing the Polar/UVI data. This work was supported by the National Natural Science Foundation of China (Grant no. 41674154) and Fundamental Research Funds for the Central Universities (Grant no. WK2080000077).

References

1 Feldstein Y I. Some problems concerning the morphology of auroras and magnetic disturbances at high latitudes. Geomagn Aeron, 1963, 3: 183
2 Feldstein Y I, Starkov G V. Dynamics of auroral belt and polar geomagnetic disturbances. Planet Space Sci, 1967, 15(2): 209–229
3 Feldstein Y I. Auroral oval. J Geophys Res, 1973, 78(7): 1210–1213
4 Liou K, Newell P T, Meng C I, et al. Synoptic auroral distribution: A survey using Polar ultraviolet imagery. J Geophys Res, 1997, 102(A12): 27197–27206
5 Liou K, Newell P T, Meng C I. Seasonal effects on auroral particle acceleration and precipitation. J Geophys Res, 2001, 106(A4): 5531-5542
6 Newell P T, Kan L, Sotirelis T, et al. Auroral precipitation power during substorms: A Polar UV Imager-based superposed epoch analysis. J Geophys Res, 2001, 106(A12): 28885–28896
7 Shue J H, Newell P T, Liou K, et al. Influence of interplanetary

magnetic field on global auroral patterns. J Geophys Res, 2001, 106(A4): 5913–5926

8 Newell P T, Kan L, Meng C I, et al. Dynamics of double-theta aurora: Polar UVI study of January 10-11, 1997. J Geophys Res, 1999, 104(A1): 95–104

9 Østgaard N, Mende S B, Frey H U, et al. Observations of non-conjugate theta aurora. Geophys Res Lett, 2003, 30(21): 2125

10 Liou K, Takahashi K, Newell P T, et al. Polar Ultraviolet Imager observations of solar wind-driven ULF auroral pulsations. Geophys Res Lett, 2008, 35(16):797-801, L16101

11 Torr M R, Torr D G, Zukic M, et al. A far ultraviolet imager for the international solar-terrestrial physics mission. Space Sci Rev, 1995, 71(1): 329–383

12 Prinz D K, Meier R R. Ogo-4 observation of the Lyman-Birge-Hopfield emission in the day airglow. J Geophys Res, 1971, 76(25): 6146–6158

Call for Paper for Two Special Issues in 2018

Dear Colleagues,

Advances in Polar Science (APS) is an international, peer-reviewed and open-access journal jointly sponsored by the Polar Research Institute of China (PRIC) and the Chinese Arctic and Antarctic Administration. It is a quarterly journal published in March, June, September and December, and circulated internationally (ISSN 1674-9928, CN 31-2050/P). Articles published in APS are free of charge with generous funding from PRIC. For more details, please visit the APS's websites: www.aps-polar.org.

In the next few years, APS is planning to publish several special issues. In 2018, two special issues entitled "Antarctic Geological Research Based on Chinese Survey Projects" or "AFoPS 2017 Annual Seminar" were proposed to be published as general issues. We would like to invite you to submit manuscripts to the two special issues.

Submitted manuscripts, except for review papers, should be complete and adequately supported by original investigation; they should not be versions of communications submitted or published elsewhere. All manuscripts will undergo regular review by members of the Editorial Board and other appropriate experts.

We thank you in advance for your consideration to submit manuscripts to the two special issues, and we encourage you to share this announcement broadly with interested colleagues. Any queries should be addressed to journal@pric.org.cn.

Editorial Office of *Advances in Polar Science*
15 December 2016